DIRECT FIBER MODEL VALIDATION: ORIENTATION EVOLUTION IN SIMPLE SHEAR FLOW

Sara Andrea Simon, Abrahán Bechara Senior, Tim A. Osswald
Polymer Engineering Center, University of Wisconsin-Madison

Abstract

Direct particle models are a promising tool for predicting microstructural properties of fiber reinforced composites. In order to validate our modeling approach for fiber orientation prediction, compression molded reinforced Polypropylene samples were subjected to a simple shear flow in a Sliding Plate Rheometer. Micro computed tomography was used to measure the orientation tensor for deformations up to 60 shear strain units. The fully characterized microstructure at zero shear strain was used to reproduce the initial conditions in the particle simulation. Fibers were placed in a periodic boundary cell and a flow field matching the experiment was applied. Samples created with the proposed compression molding technique showed repeatable and controlled initial orientation. The model showed good agreement with the steady state orientation; however, it showed a faster orientation evolution at the start of the shearing process.

Introduction

Computational tools to simulate the processing of fiber reinforced composites have become indispensable for the automotive industry. The ability to accurately predict the microstructure of molded components is a key factor not only for design calculations but also for addressing issues such as shrinkage and warpage before mold fabrication. Almost all commercially implemented models (Folgar-Tucker, Anisotropy Rotary Diffusion (ARD) Reduced Strain Closure (RSC)) use experimentally determined fitting parameters. However, these experiments are costly, lengthy and limited in the amount of information they can provide.

Particle level simulations have been used in the past to aid in the understanding of these type of systems [1, 2]**.** In these simulations, each fiber is modeled individually as a chain of rigid elements. Fibers are placed in a predetermined flow field and hydrodynamic forces, as well as fiber-fiber interactions, are computed to predict fiber motion [3, 4].

Obtaining parameters numerically has advantages over obtaining them experimentally. In a numerical setup, all parameters can be accurately controlled, detailed information is always available and the simulations are relatively inexpensive to perform. An additional advantage of these models is the high accuracy that is reached by modeling the actual motion of individual fibers [5].

The objective of this paper is to provide reliable fiber orientation evolution data in a well-defined simple shear flow to aid in the validation and development of a multi-particle model for reinforcing fibers. Simple shear was chosen since it is one of the fundamental flow conditions present in most polymer processes. Selecting it allows us to directly correlate the rate of deformation with the filler's behavior. Compression molded glass fiber-reinforced polypropylene samples were sheared in a Sliding Plate Rheometer following Cieslinski et al. [6]. As has been shown by the same author, compression molding is not a suitable sample preparation method since it has no control over the planar orientation of the fibers. In this work, we will therefore present a compression molding technique which ensures a controlled and repeatable initial fiber orientation for shear experiments. Results from both simulation and experiment are compared.

Experimental

Sample preparation

The material used in this work was a commercially available glass fiber-reinforced polypropylene with 20 %wt. fiber content (SABIC®, STAMAX 20YM240). The material properties are listed in Table 1.

Table 1: SABIC® STAMAX 20YM240 material properties.

Material Property	Value
Nominal Fiber Density [%vol]	8.2
Nominal Fiber Length [mm]	15
Fiber Diameter [µm]	19±1
Density of Fibers [g/cm^3]	2.55
Density of Composite [g/cm^3]	1.04
Density of Polypropylene [g/cm^3]	0.91

Samples for the sliding plate rheometer (SPR) were prepared by compression molding extruded strands. Compression molding was chosen as the sample preparation method to obtain a simple, repeatable and controlled initial fiber orientation (FO). Starting with identic initial FO is important to accurately validate the proposed direct fiber model. Previous work [6, 7] has shown that samples created with injection molding also provide a repeatable initial FO, however, injection molded specimen show a more complex core shell structure [8], which is it difficult to reproduce computationally.

The material was received as 15 mm long pellets created through a pultrusion process where the length of the fibers is identical to the pellet length. This means that fibers are not dispersed within the matrix. In order to disperse the fibers, the material was first processed in an Extrudex Kunststoffmaschinen single screw extruder with a smooth barrel (EDN 45X30D). The 45 mm 30 L/D extruder was equipped with a gradually tapering screw and a 3 mm die. The processing settings were based on the processing guidelines provided by SABIC®. The seven temperature zones of the extruder were set to 210, 210, 220, 220, 230, 230 and 230 °C, respectively. The composite was extruded at 5 rpm. The extrudates were pulled by a Conair precision puller to ensure homogenous strands.

Due to the low extrusion speed, most of the initial fiber length (FL) was maintained after processing, giving a number average fiber length (L_N) of 6.7 mm and a weight average fiber length (L_W) of 11.4 mm. The maximum detected FL showed the initial pellet length of 15 mm. The FL measurements follow the method developed at the Polymer Engineering Center and will be described in the following chapter.

Computational time for the mechanistic model simulation is geometrically proportional to the maximum detected FL. In order to reduce computation, the strands were pelletized to 3.2 mm. Initial trials showed that alignment of pellets in the mold did not yield a repeatable initial FO as, during compression, pellets could move easily and rotate. Therefore, pellets were re-extruded

and strands were cut to the mold dimensions. Analysis of the strands showed a L_N of 0.83 mm and L_W of 1.53 mm and a maximum detected FL of 4 mm. The mold geometry used in this study was a rectangular prism (14 mm x 14 mm x 2.1 mm).

The top and the bottom of the mold were coated with aluminum foil to facilitate sample extraction. The bottom half of the mold was placed on a heating plate to cause partial melting of the aligned strands (Figure 1a, 1b). The resulting plate was flipped and re-molten; this second step was needed to remove air bubbles caught between strands.

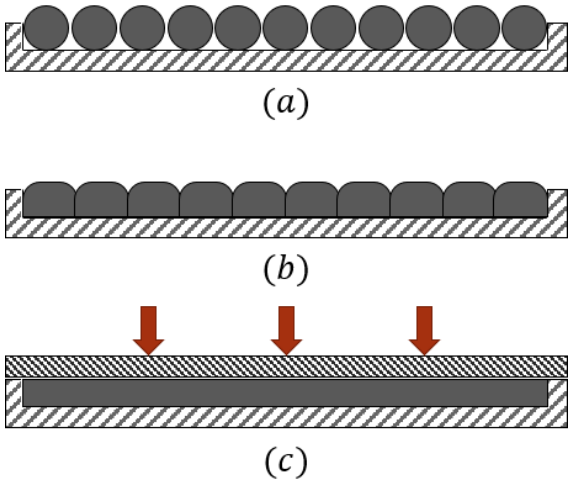

Figure 1: Sample preparation steps. (a) alignment of strands, (b) partial melting of strands, (c) compression molding.

The plates were then compression molded with a Carver compression molding machine (Model 3889.1NE1000) (Figure 1c). The two platens were heated to 210 °C and a load of 1000 lbs was applied for 2 minutes. After compression, the plates were sandwiched between two cold steel plates to prevent warpage. The fiber properties (FO, FL and fiber density distribution) of the final plates were analyzed and the results are summarized in Table 2. Multiple samples were taken within a compression molded plate to ensure homogeneity.

Table 2: Average fiber properties of compression molded plates, with a_{11} (extrusion direction), a_{22} and a_{33} as the orientation tensors.

Material Property	Value
a_{11} [-]	0.86
a_{22} [-]	0.11
a_{33} [-]	0.03
Fiber concentration [%vol]	7.93
L_N [mm]	0.83
L_W [mm]	1.53

Sliding Plate experiment

FO evolution as a function of shear strain was determined by shearing compression molded samples in a SPR under a controlled simple shear flow. The SPR was based on the design of Giacomin et al. [9]. This rheometer was chosen over a rotational rheometer to overcome curvature effects observed in previous work [6]. The SPR rheometer used in this study is shown in Figure 2.

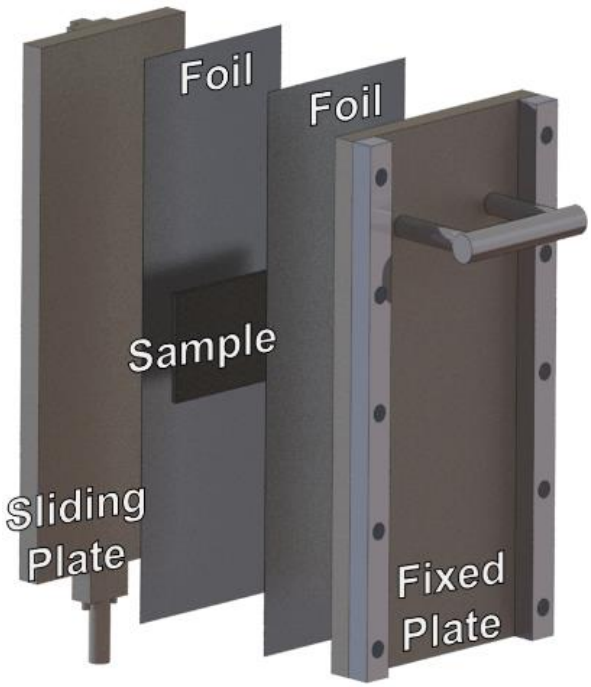

Figure 2: Sliding Plate Rheometer assembly.

The SPR has an effective surface of 100 x 300 mm^2, a maximum stroke of 120 mm and a gap size of 2 mm. The maximum displacement and the fixed gap size limit the deformation that can be imposed on the sample to a maximum shear strain of 60. The SPR rests inside a forced convection oven and the sliding plate is moved by an Interlaken 3300 test frame.

The experimental procedure is based on Cieslinski et al. [6]. The rheometer was heated to 260 °C for 2 hours prior to sample loading. Upon loading, the test specimen was rotated 90° with respect to the extrusion direction, effectively swapping the a_{11} with the a_{22} tensor. This was done to have the experiment start with a low alignment in the shearing direction so a larger change in orientation could be observed. The samples were secured between the rheometer plates and allowed to melt evenly before tightening the screws to a final gap of 2 mm (Figure 3a). Since the initial thickness of the compression molded plates was 2.1 mm, the sample was slightly compressed when tightening the plates to guarantee full contact. After an additional 10 minutes of heating the sample was sheared at a rate of 1 s^{-1} (Figure 3b). Forced convection was used to accelerate the cooling of the sample in the rheometer to preserve its shape and FO. Once room temperature was reached, the sample was extracted and cut for analysis (Figure 3c). Six repetitions per testing condition were used to ensure accuracy and repeatability of results.

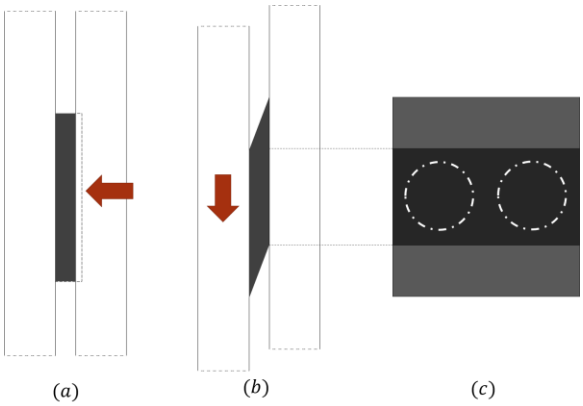

Figure 3: Sliding Plate Rheometer procedure, (a) Compression of molten sample during loading, (b) shearing of sample, (c) sample extraction for fiber orientation analysis; dark region represents area of pure shear.

Measurement of fiber microstructure

A fully characterized microstructure is required to accurately reproduce the initial conditions in the mechanistic model simulation. The in-plane microstructure analysis involved determining the fiber concentration as well as the fiber length. Analysis of the thickness-wise microstructure included determining the fiber volume fraction and the fiber orientation. A detailed description of the employed analysis techniques is given in the following paragraphs.

Fiber Orientation Characterization

FO was measured by using the micro computed tomography (µCT) technology approach (Figure 4). For the measurement an X-ray source illuminated the specimen which was fixed on a rotating platform. The X-rays passed through the sample and were attenuated by the material. Depending on the configuration of the constituents of the sample, the energy of the X-rays was absorbed differently. A detector recorded the attenuated X-rays as radiographs at each predetermined angle. A full 3D representation of the sample was generated by all radiographs [8, 10]. The µCT data set was then further processed by using the VG StudioMAX (Volume Graphics) software. This software has an implemented tool for FO analysis and quantifies the FO using the structure tensor approach [11].

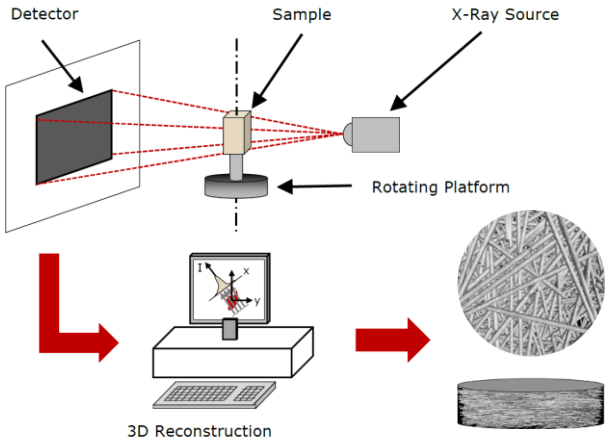

Figure 4: Schematic of the micro computed tomography system used in this study. Image was adapted from [8].

Samples were scanned with a Metrotom 800 µCT system (Carl Zeiss AG). The used scan parameters are summarized in Table 3.

Table 3: Micro computed tomography settings.

Parameter	Value
Voltage [V]	80
Current [A]	100
Integration Time [ms]	1000
Gain [-]	8
Voxel Size [µm]	3.5
Number of projections [-]	2200

Fiber Length Characterization

The FL was determined by using the FL measurement concept developed at the Polymer Engineering Center, UW-Madison. This technique consists of a time-efficient dispersion system and a fully automated image-processing algorithm to measure a large amount of fibers.

As even small samples might contain several million fibers this measurement technique applies a downsampling step based on the method proposed by Kunc et al. [12]. Coupons were cut out, transferred into specially designed perforated brass sample holders and a weight was put on top. The container and the added weight act as a constraint to help to maintain the original sample size and prevent the fiber network from expanding during pyrolysis. The polymer matrix was burned off for a period of 2 hours at 500 °C. To obtain a sub-sample of the ashed fibers a hypodermic needle was centrically inserted through a needle guide into the fiber network and a column of resin was injected. The resin was cured with a LED Flashlight. A second burn-off for a period of 1.5 hours at 500 °C was performed to remove the resin [12, 13].

As a next step the fibers were dispersed through an air dispersion chamber using bursts of compressed air at 1.5 bar. Due to the turbulences in the enclosed system a disentanglement and a uniform dispersion of the fibers on glass plates can be achieved. The fibers were then scanned at 2400 dpi. The scanned image was processed and enhanced in Photoshop. A binary image was created by using a thresholding technique.

The Marching Ball image processing algorithm was employed in this work as it automatically detects single fibers and quantifies the fiber length distribution (FLD). The algorithm can identify bent as well as intersecting fibers, which is particularly important for long fiber reinforced composites. At least 30,000 fibers were analyzed for each sample.

It is known that down-sampling methods result in skewing the FLD. Thus, the Kunc correction function was used for all FL values to provide an unbiased FLD (Equation 1).

$$N(L) = \Phi(L)\left(1 + \frac{4L}{\pi d}\right)^{-1}$$

Equation 1: Corrected number of fibers of a certain length N(L), where Φ(L) is the number of fibers of length L and d the diameter of the glue column, respectively [12].

The output of the analysis is a data set consisting of the individual lengths of all fibers. This raw data set needs to be statistically processed in order to obtain comparable results, such as the FLD, L_N and L_W. The FLD and the average values can be calculated according to equation 2-4.

$$W(L_i) = P(l \leq L_i) = \sum_{i=0}^{L_i} \frac{N_i}{n}$$

Equation 2: Cumulative FLD W, which gives the probability that fibers of length l are shorter than a certain value L_i. W is calculated by summating the relative frequency of each length interval (quotient of the number of fibers of a certain length N_i divided by the total number of fibers n) [10].

$$L_N = \frac{\sum_i N_i l_i}{\sum_i N_i}$$

Equation 3: Number average FL, L_N. The lengths l_i span the range of the data. N_i is the number of fibers with lengths between l_i-Δl/2 and l_i+Δl/2 (Δl is the experimental bin width and a set of length values l_i such that l_i+1=l_i+Δl) [10, 14, 15, 16].

$$L_W = \frac{\sum N_i\, l_i^2}{\sum N_i\, l_i}$$

Equation 4: Weight average FL, L_W. The lengths l_i span the range of the data. N_i is the number of fibers with lengths between l_i-Δl/2 and l_i+Δl/2 (Δl is the experimental bin width and a set of length values l_i such that l_i+1=l_i+Δl) [10, 14, 15, 16].

Fiber Concentration Characterization

The local fiber density was obtained by determining the fiber weight fraction through pyrolysis at a temperature of 500 °C for 2 hours. The specimen was weighed before and after pyrolysis and the fiber volume fraction was determined according to Equation 5:

$$V_f = \frac{v_f}{v_c} \times 100$$

Equation 5: Fiber volume fraction V_f in %vol, with v_f as the volume of the fiber in g/cm³ and v_c as the volume of the composite material in g/cm³, respectively.

This method is a quick and effective way to determine the average fiber volume fraction, but it does not give any information on the fiber concentration (FC) in each layer of the sample. Pyrolysis can also be used to study the FC in the thickness direction. However, this approach requires the collection of material of several sample layers through the thickness. For each data point the sample would need to be prepared by grinding. As has been reported in literature, this approach is not only cumbersome and time consuming, but also leads to errors in analysis [8].

We will therefore use the µCT approach to determine the fiber density through sample thickness. The layer wise FC was quantified with VG StudioMAX (Volume Graphics) software. In this approach the µCT data set is converted into a stack of 2D cross-sectional images aligned normal to the thickness direction. These grayscale images are transformed into binary images by thresholding, which separates the image into black (matrix) and white (fibers) pixels. Subsequently, the fiber volume fraction through the thickness is calculated [8].

Modeling and Simulation

Single Particle Model

The computational model, subject of this study, is based on the work done by Schmid et al. [17]. Each fiber is represented by a chain of rigid segments connected with spherical joints. Particle inertia is neglected in anticipation of the low Reynolds numbers characteristic of viscous suspensions. Extensional and torsional deformations are neglected as well. There is no Brownian motion and no buoyant effects.

As shown in Figure 5a, a segment is hydrodynamically represented as a chain of beads. The force (F^i) and torque (T^i) exerted by the fluid on an individual segment are computed through the hydrodynamic force (F^k) and torque (T^k) acting on spheres located along the segment's axis (r_k).

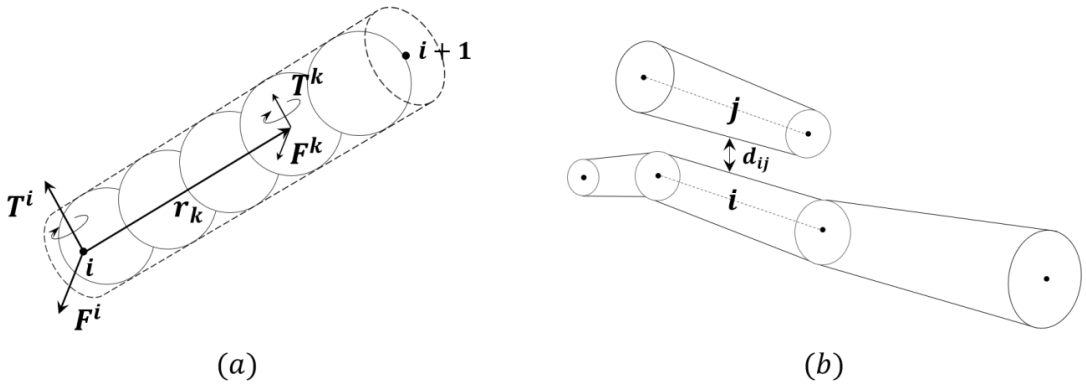

Figure 5: (a) Hydrodynamic representation of segments, (b) Fiber interaction is depicted. The contact force is different than zero when $d_{ij} < D$ [3].

The contact force between fibers is treated with a discrete penalty method. Penalty methods work by detecting proximity between colliding objects and applying a repulsive "penalty" fo rce when the distance (d_{ij}) to the collision target is small, increasing the strength of repulsion force as distance decreases (Figure 5b).

After defining the rules of motion for a single fiber, a simulation can be set up by placing a representative number of fibers in a unit cell and imposing a flow field (Figure 6). Periodic conditions are defined in the boundaries perpendicular to the flow direction in order to guarantee a constant fiber volume fraction. Fibers exiting through these boundaries are cloned as reent ering fibers. “Ghost” cells are placed adjacent to the periodic boundaries to maintain continuity in the force calculation (Figure 6).

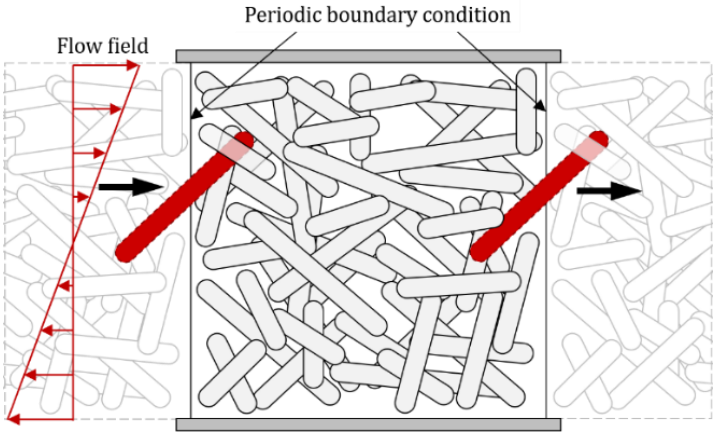

Figure 6: Unit cell with periodic boundary conditions. Image adapted from [3].

Reproducing Initial Conditions

As noted by Cieslinski et al. [6] accurate and repeatable initial conditions are needed for obtaining reliable rheological data. For this purpose, the microstructure of the experimental samples was carefully characterized and used to generate a matching cluster of fibers for the simulation. In the pre-processing stage of the simulation, global values of orientation (a_{ij}), fiber density (%vol) and average fiber length (L_N, L_W) can be assigned to a cluster of fibers. Since the experimental samples do not show homogeneous microstructure through the thickness, a discrete approach must be taken in order to reproduce these characteristics.

Discretization of Fiber Density and Fiber Orientation

µCT analysis generates a continuous set of fiber volume fraction and orientation tensors across the thickness of the sample; this thickness was discretized into 10 segments (Δt=0.2 mm) and the continuous values were averaged per each segment as shown in Figure 7 and Figure 8.

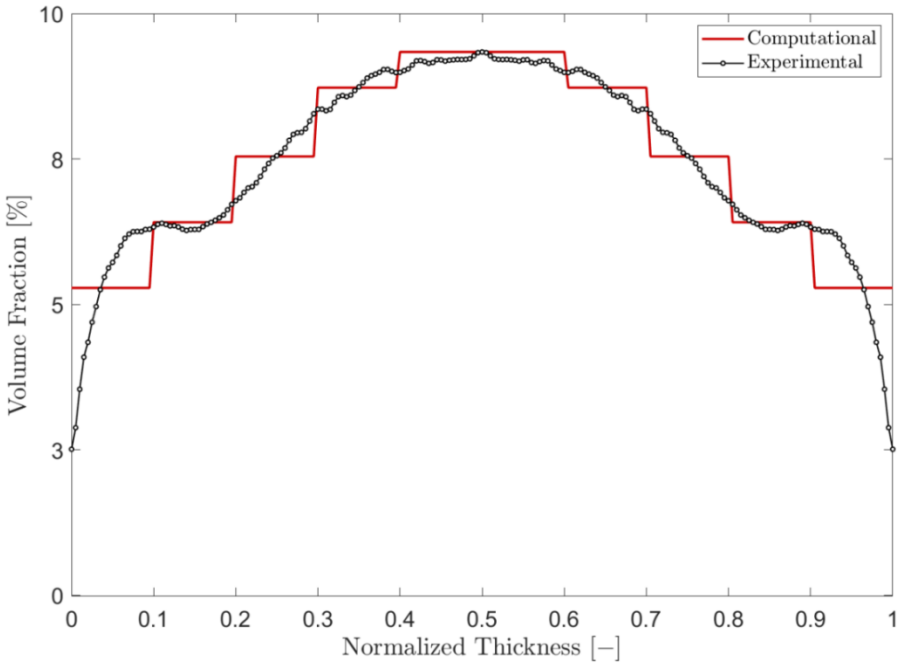

Figure 7: Discretization of fiber concentration through thickness.

It is worth noticing that the maximum number of segments that can be used is limited by the a_{33} component of orientation. As the thickness of the individual clusters reduces, achieving a desired value of orientation in that direction becomes unattainable.

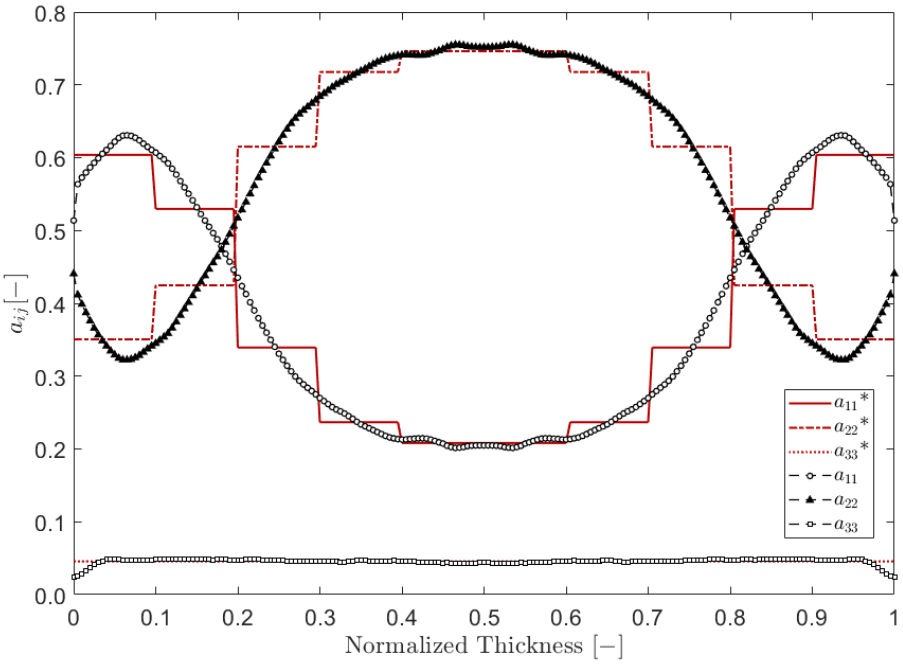

Figure 8: Discretization of fiber orientation through thickness.

Average Fiber Length Reproduction

The experimental FL is given in the form of number and weight averages (L_N 0.83 mm, L_W 1.53 mm). The cell's volume and the global fiber volume fraction are used to calculate the cumulative length of the fibers. This cumulative length is then broken down into individual length bins until the length distribution averages match the experimental values (Figure 9a).

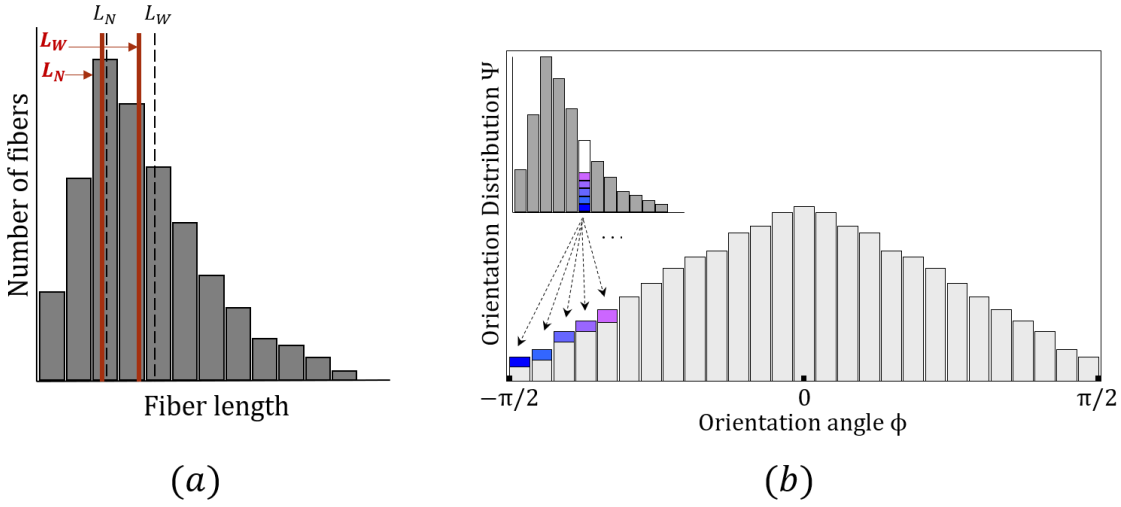

Figure 9: (a) Length distribution function and experimental averages (red). (b) Length assignment to orientation distribution.

When placing the fibers inside the unit cell, fibers of same length are distributed equally among the individual angle bins, thus guaranteeing equal length representation for every orientation (Figure 9b). Longer fibers start populating the cell first, then progressively shorter fibers fill in the remaining volume until the desired volume fraction is achieved.

Finally, all individual clusters are stacked in the same sequence as the discretized data to create the complete microstructure as shown in Figure 10.

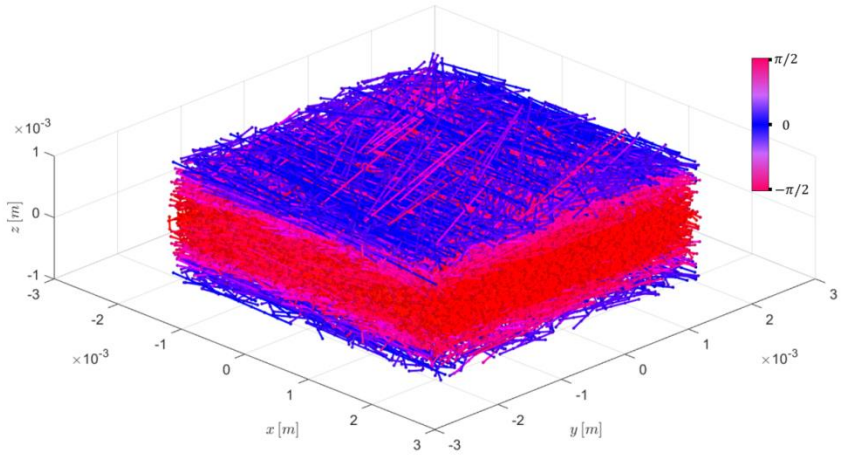

Figure 10: Computational cluster, with x as the shearing direction.

Simulation

To match the experimental conditions, a simple shear flow field was imposed on the unit cell with a rate of deformation of 1 s^{-1}. The viscosity was calculated using the experimental temperature, rate of deformation and properties of the neat polypropylene. The dimensions of the cell are dictated by the sliding plate gap in Z direction of 2 mm and the maximum FL of 4 mm. In order to allow free rotation, the dimension in X and Y were set to 1.1 x the maximum FL. The simulation time was set to 60 seconds to reach the total deformation of 60. Cell walls parallel to planes XZ and YZ have a periodic boundary condition. A tight array of static fibers was placed on the upper and lower boundaries to emulate the SPR walls. The simulation outputs the nodal coordinates of each fiber at every time step. With this information both global and thickness wise orientation tensors can be calculated.

After the sliding plate was tightened to the final gap thickness of 2 mm the orientation tensors changed from the values reported in Table 2. The actual values corresponding to the initial conditions are listed in Table 4.

Table 4: Experimental and computational orientation tensors used to reproduce initial conditions.

Material Property	Experimental	Computational
a_{11} [-]	0.36	0.36
a_{22} [-]	0.59	0.62
a_{33} [-]	0.05	0.02

Results and Discussion

Global diagonal components of the orientation tensor as a function of shear strain are shown in Figure 11. The a_{11} component starts at 0.36 and transitions to a steady state value of around 0.7 for both the experiment and the simulation. The steady state is reached at a total strain of 50, again, for both cases. Since this material falls in the category of long fiber composites, values of a_{33} component are expected to be low since long fibers will orient mostly on the XY plane. Experimental values at zero strain show a low standard deviation which demonstrates a repeatable initial FO, validating the sample preparation method.

From the start, the simulation shows faster orientation evolution than the experiment. This phenomenon has also been reported in literature [18] for other diffusion models. Jeffrey's Hydrodynamic model is based on Jeffrey's equation for the motion of a single fiber which was later modified with an isotropic rotary diffusion term to account for fiber-fiber interactions. It has been proven that this model always predicts faster orientation kinetics in a transient state when compared to related experiments. This issue was addressed by combining the Hydrodynamic model with the ARD model. However, results still showed the initial quicker rate of orientation [18]. To treat this fast response problem of orientation, Wang et al. [19] developed a new evolution equation of the second orientation tensor and named his model the RSC model. This model still shows a slightly quicker initial rise of flow-direction orientation (a_{11}) but achieves nearly the same steady orientation states as obtained with experiments [18]. A recent study by Mezi et al. [20] addresses a current issue with direct particle approaches, namely, the missing coupling between particle and fluid i.e. the models only consider hydrodynamic forces acting on the particles but not

the effect of particles on the surrounding fluid. When the effect of particle motion on the flow field is accounted for, the effective shear rate decreases in value leading to a slower orientation evolution. However, implementing this coupling is extremely costly computationally, therefore it was not implemented in this work.

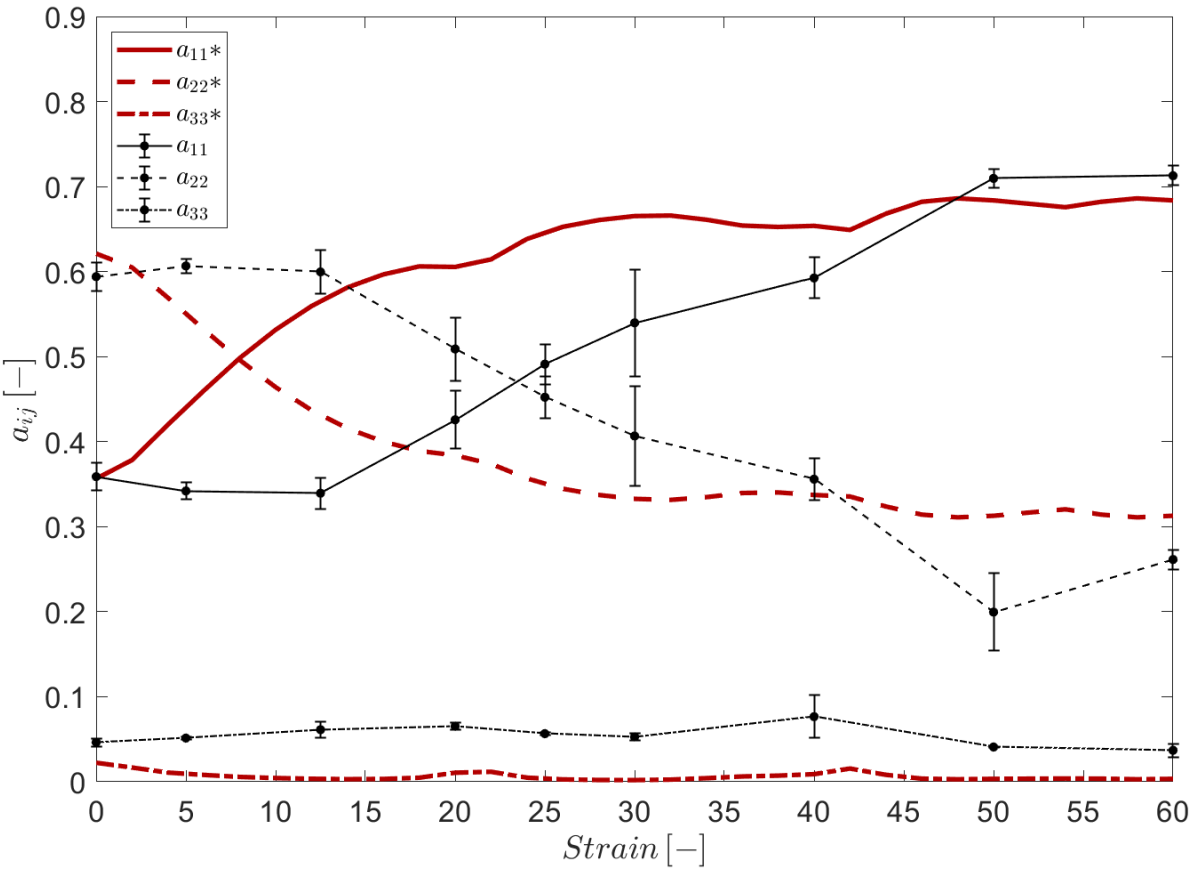

Figure 11: Experimental (black) and predicted (red) fiber orientation evolution.

The experimental core-shell structure is largely unchanged at 12.5 strain units when compared to the initial orientation (Figure 12). At the same applied strain, the simulation already shows a large transition to a rather homogenous structure. This once again shows that the direct particle model exhibits a faster orientation evolution. Once 60 strain units are reached, the core-shell profile disappears and a good match between experiment and simulation can be observed. It is assumed that shearing beyond 60 strain units would lead to fiber orientations which would be constant throughout the thickness demonstrating a steady state FO [6].

The simulation results for a_{11} through thickness were smoothed and plotted for different strains in Figure 13. Under a constant shear the heterogeneous orientation profile transitions into a homogeneous steady state. The most significant change in orientation occurs in the core of the sample. The rate of change slows down as orientation approaches steady state. This aligns with results published in literature [6] as well as previous work with injection molded plaques [7].

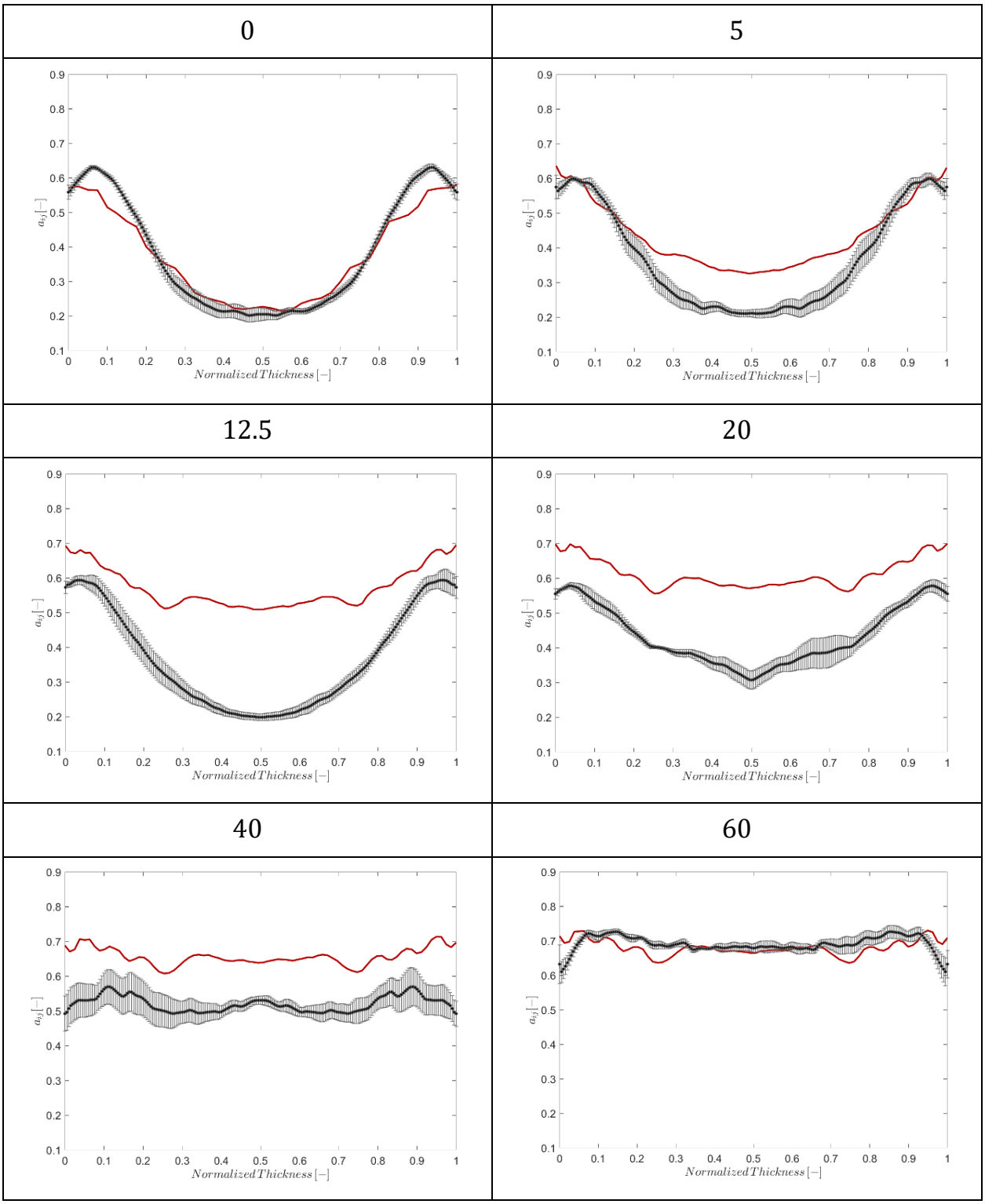

Figure 12: Experimental (black) and predicted (red) a_{11} values through sample thickness at varying shear strains.

μ-CT data (Figure 14) also shows fiber alignment in the flow direction and underlines the trend seen in Figure 13. The green/blue regions demonstrate fibers which are aligned with the

flow direction, characterized by large values of a_{11} and low values of a_{22}, whereas red regions represent a crossflow orientation state, with low values of a_{11} and high values of a_{22}. Yellow indicates fibers which are oriented in the thickness direction (a_{33}). This color is almost absent in Figure 14 which indicates a nearly planar orientation state [18]. The clearly define core-shell structure becomes homogeneous after shearing.

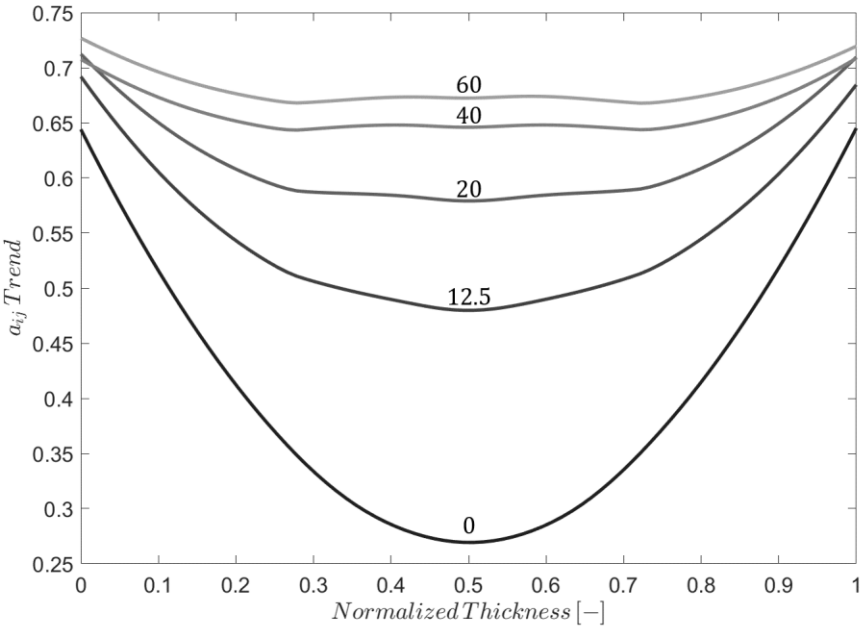

Figure 13: Smoothed computational a_{11} evolution.

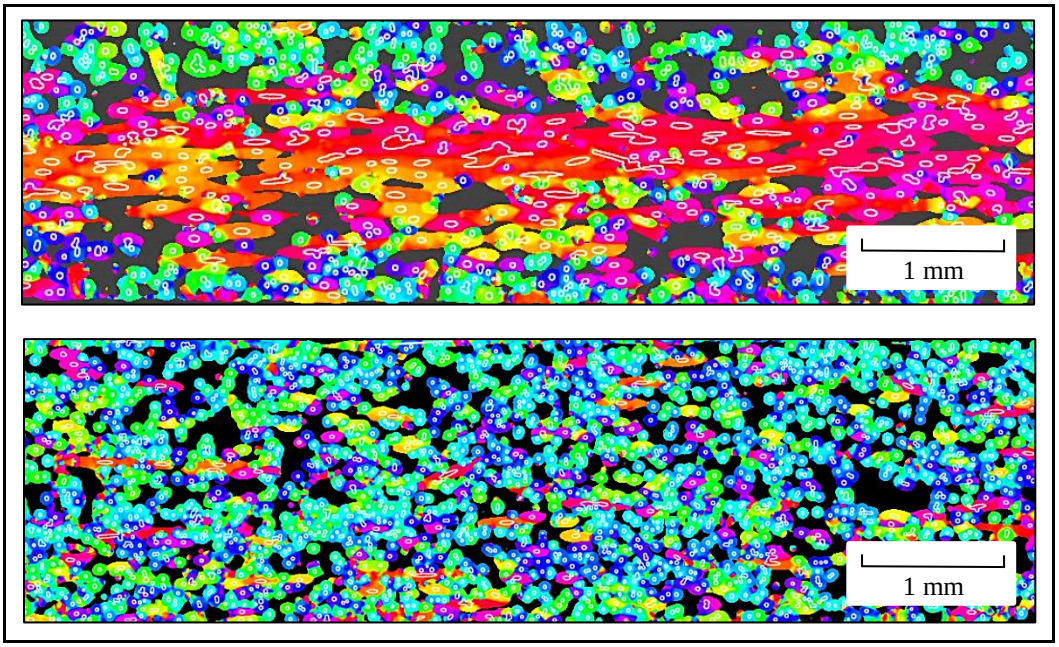

Figure 14: µCT FO through thickness from VG StudioMax analysis, top: 0 shear strain, bottom: 60 shear strain.

Conclusions and Outlook

A particle-level simulation for reinforcing fibers was successfully used to determine the FO evolution. Results showed good agreement with the steady state orientation tensor. In its current state the model can be employed for two main tasks: firstly, the periodic boundary cell can be used as a numerical rheometer, where correlations between process parameters and fiber properties are established. This is especially useful for determining fitting parameters for commercially implemented continuum models [1]. Secondly, the model can be coupled with mold filling simulations in order to study fiber motion and fiber-mold interaction in small scale geometries; for example, fiber matrix separation during rib filling [2] or FO in the flow front [21].

A reliable method for preparation of samples for suspension rheology was developed. Repeatable and controlled initial orientation can be achieved through the presented compression molding technique.

Next steps of this project include:

1. Reproducing further experiments conducted by Cieslinski et al. [6] with different FC to evaluate the impact of coupling in the direct fiber model.
2. Repeating the study with an extensional flow to gain insight on this fundamental type of flow.
3. Predicting the FO evolution with currently employed diffusion models which are based on the orientation tensor scale to evaluate how the mechanistic model performs.

This future work will be used to evaluate the model and aid in its development. Additionally, a better understanding of the underlying physics of the motion of fibers and their interaction in concentrated regimes can be gained.

Acknowledgements

This material is based upon work supported by the National Science Foundation under Grant No. 1633967. The authors would like to thank SABIC® for their continuous support and collaboration with our research group and their material supply. Additionally, we would also like to thank our colleagues from the Polymer Engineering Center who provided insight and expertise that greatly assisted the research.

Bibliography

[1] C. Perez, "Particel level simulation of fiber motion to determine continuum based models parameters for fiber orientation prediction," in *ECCM17 - 17th European Conference on Composite Materials*, Munich, 2016.

[2] C. Kuhn, "Simulative Prediction of Fiber-Matrix Separation in Rib Filling During Compression Molding Using a Direct Fiber Simulation," *Journal of Composites Science,* vol. 2, no. 1, 2018.

[3] C. Perez, "The use of a direct particle simulation to predict fiber motion in polymer processing," *Dissertation - University of Wisconsin-Madison,* 2016 .

[4] E. Baur, S. Goris, D. Ramirez, P. Schmidtke and T. Osswald, "Mechanistic model to determine fiber orientation simulation material parameters," *Proceedings of the Annual Technical Conference of the Society of Plastics Engineers, Las Vegas, NV,* 2014.

[5] U. Strautins, "Flow-driven orientation dynamics in two classes of fibre suspensions," *Dissertation - Fachbereich Mathematic der Technischen Universität Kaiserslauten,* 2008.

[6] M. J. Cieslinski and D. Baird, "Obtaining repeatable initial fiber orientation for the transient rheology of fiber suspensions in simple shear flow," *Journal of Rheology,* pp. 161-174, 2015.

[7] S. Simon, A. Bechara Senior and T. Osswald, *Predicting Fiber Orientation Evolution using Particle-level Simulation: An Experimental Validation,* Poster at Automotive Composites Conference & Exhibition, 2018.

[8] S. Goris, "Characterization of the process-induced fiber configuration of long glass fiber-reinforced thermoplastics," *Dissertation, University of Wisconsin-Madison,* 2017.

[9] A. Giacomin and J. Dealy, "A novel sliding plate rheometer for molten plastics," *Polymer Eningeering Science,* vol. 29, pp. 499-504, 1989.

[10] B. N. Nguyen, S. Bapanapalli, J. Holbery, M. Smith, V. Kunc, B. Frame, J. Phelps and C. Tucker, "Fiber length and orientation in long fiber injection molded thermoplastics," *Journal of Composite Materials,* vol. 42, no. 10:1003, 2008.

[11] M. Krause, B. Hausherr, C. Burgeth and W. Krenkel, "Determination of the fibre orientation in composites using the structure tensor and local X-ray transform," *Journal of Materials Science,* vol. 45, no. 4, p. 888, 2009.

[12] V. Kunc, B. Frame, B. Nguyen and G. Velez-Garcia, "Fiber length distribution measurement for long glass and carbon fiber reinforced injection molded thermoplastics," in *7th Annual Society of Plastic Engineers Automotive Composites Conference & Exhibition*, MI, Troy, 2007.

[13] J. Phelps, A. El-Rahman and V. Kunc, "A model for fiber length attrition in injection-molded long-fiber composites," *Composites Part A,* pp. 11-21, 2013.

[14] U. Yilmazer and M. Cansever, "Effects of processing conditions on the fiber length distribution and mechanical properties of glass fibre reinforced nylon-6," *Polymer Composites,* vol. 23, no. No. 1, 2002.

[15] P. Ren and G. Dai, "Fiber dispersion and breakage in deep screw channel during processing of long-fiber reinforced polypropylene," *Fibers and Polymers,* vol. 15, pp. 1507-1516, 2014.

[16] J. Wang, C. Geng, F. Luo, Y. Liu, K. Wang, Q. Fu and B. He, "Shear induced fiber orientation, fiber breakage and matrix molecular orientation in long glass fiber reinforced polypropylene composites," *Materials Science and Engineering A,* pp. 3169-3176.

[17] C. Schmid, L. Switzer and D. Klingenberg, "Simulations of fiber flocculation: effects of fiber properties and interfiber friction," *Journal of Rheology,* vol. 44, pp. 781-809, 2000.

[18] M. Wang, R. Chang and C. Hsu, Molding Simulation: Theory and Practice, Carl Hanser Verlag, 2018.

[19] J. Wang, R. Chang and C. Hsu, "An objective model for slow orientation kinetics in concentrated fiber suspensions: Theory and Rheological evidence," *Journal of Rheology,* vol. 52, pp. 1179-1200, 2016.

[20] D. Mezi, "Fiber suspension in 2D nonhomogeneous flow: The effects of flow/fiber coupling," *Journal of Rheology,* vol. 63, no. 3, pp. 405-418, 2019.

[21] A. Bechara, S. Kollert, J. Onken, D. Ramirez and T. Osswald, "Effect of fountain flow on fiber orientation and distribution in fiber filled polymers during mold filling," in *ANTEC*, Las Vegas, 2013.